bioRxiv preprint doi: https://doi.org/10.64898/2026.06.04.730071; this version posted June 8, 2026. The copyright holder for this preprint (which was not certified by peer review) is the author/funder, who has granted bioRxiv a license to display the preprint in perpetuity. It is made available under a CC-BY 4.0 International license.

Title: Antidepressant fluoxetine engages astrocytic cAMP via purinergic signalling

Authors

Catriona Marston[1], Kratika Mujmer[1], Bárbara Vaccari Cardoso[1,2], Sergey Kasparov[1], Anja G Teschemacher[1], Valentina Mosienko[1]

Affiliations

[1]School of Psychology and Neuroscience, University of Bristol, Bristol, UK

[2]current affiliation: Domainex Ltd., Cambridge, United Kingdom

Corresponding author: Dr Valentina Mosienko (valentina.mosienko@bristol.ac.uk)

School of Psychology and Neuroscience

University of Bristol

University Walk, BS8 1TD

Bristol, UK

Data availability statement: Data will be made available upon request to authors

Funding statement: The financial support was provided by AMS Springboard award SBF005\1102 and the MRC Career Development Award MR/T031115/1 to VM

Conflicts of interest: The authors report no conflicts of interest.

Number of words: 4137

Number of figures: 4 main figures, 1 supplementary figure

Number of tables: 3 supplementary

bioRxiv preprint doi: https://doi.org/10.64898/2026.06.04.730071; this version posted June 8, 2026. The copyright holder for this preprint (which was not certified by peer review) is the author/funder, who has granted bioRxiv a license to display the preprint in perpetuity. It is made available under a CC-BY 4.0 International license.

Abstract

The use of selective serotonin reuptake inhibitors (SSRIs), the first-line treatment for depression, has increased by about 50% over the past decade, placing them amongst the top 10 most frequently prescribed drug classes globally. Overall, SSRIs are effective in reducing frequency, severity, and duration of depressive episodes for a majority of patients, yet the mechanisms underlying their therapeutic effects are not fully understood. While SSRIs elevate synaptic serotonin, this action alone cannot account for their therapeutic effects. Additionally, SSRIs engage astrocytes, enhancing cyclic adenosine monophosphate (cAMP) signalling which is reported to be downregulated in depression. However, the signalling mechanisms underlying SSRI-induced upregulation of the astrocytic cAMP pathway remain unclear. Here, we identify a cascade of events by which the SSRI fluoxetine elevates intracellular cAMP levels in astrocytes, a process that depends on astrocyte-microglia crosstalk and purinergic signalling. Using FRET-based sensors in primary rat astrocytes, we show that fluoxetine elevates intracellular cAMP by 28% without altering calcium dynamics. cAMP increase was blocked by both serotonin (5-HT) 2B and adenosine 2B (A2B) receptor antagonists. Using the GRAB-ATP1.0 sensor and luminescence assays, we revealed that fluoxetine enhances astrocytic ATP release by 10% in a 5-HT2B receptor-dependent manner. Consistent with microglia-driven conversion of extracellular ATP to adenosine, which engages astrocytic A2B receptors, depletion of microglia in astrocyte cultures diminished fluoxetine-induced cAMP elevations and increased extracellular ATP. Together, these findings reveal that fluoxetine requires glial crosstalk and coordinated purinergic signalling to enhance astrocytic cAMP, a process shown to contribute to the therapeutic effect of SSRIs.

bioRxiv preprint doi: https://doi.org/10.64898/2026.06.04.730071; this version posted June 8, 2026. The copyright holder for this preprint (which was not certified by peer review) is the author/funder, who has granted bioRxiv a license to display the preprint in perpetuity. It is made available under a CC-BY 4.0 International license.

Introduction

Selective serotonin reuptake inhibitors (SSRIs) are the first line of treatment for depressive disorders that represent, with ~5.7% of the population affected, the most common mental health condition and the leading cause of disability worldwide (1). SSRIs are amongst the top 10 most frequently prescribed drug classes (2), with prescriptions increasing by 46% over the past decade (3). SSRIs alleviate depressive symptoms in 40-60% of patients, although evaluating their efficacy is challenging due to the heterogeneity in symptom severity and clinical presentation (4,5). Overall, SSRIs are widely recognised as effective in reducing the frequency, severity, and duration of depressive episodes (6). While some studies have questioned their overall efficacy (7), findings evaluating efficacy are often limited by methodological challenges, including difficulties in measuring treatment response, the absence of reliable biomarkers, and high placebo response rates in clinical trials.

SSRIs increase extracellular concentration of serotonin (5-hydroxytryptamine, 5-HT) by inhibiting its reuptake through the neuronal serotonin transporter (SERT), a mechanism initially proposed to underlie their therapeutic effects (8). Although SSRIs exhibit high affinity for SERT, it is still debated whether this action alone mediates their clinical efficacy or represents just one component of their mechanism of action. Fluoxetine (FLX), one of the most commonly prescribed SSRIs, has high affinity for SERT ($K_i \approx 5.2 \times 10^{-8}$ M) and substantially lower affinity for other monoamine transporters, including dopamine ($\approx 10^{-5}$ M) and noradrenaline ($\approx 1.5 \times 10^{-5}$ M, (9)). However, lack of brain serotonin does not exacerbate depression-like phenotype, nor does it interfere with antidepressive effects of SSRIs in preclinical models of depression (10–12). These findings suggest that although SSRIs increase brain serotonin levels, their therapeutic effect may be mediated via mechanisms independent of 5-HT availability.

bioRxiv preprint doi: https://doi.org/10.64898/2026.06.04.730071; this version posted June 8, 2026. The copyright holder for this preprint (which was not certified by peer review) is the author/funder, who has granted bioRxiv a license to display the preprint in perpetuity. It is made available under a CC-BY 4.0 International license.

One potential alternative pathway may be the activation of 5-HT2B receptors to which FLX has fairly high affinity (5-10x10^{-6} M), and which were shown to be required for antidepressive properties of SSRIs (13,14).

SSRIs act not only on neurons but also affect astrocytes, a major population of non-neuronal cells in the brain. Evidence from post-mortem human studies and animal models of depression suggests that SSRIs reverse reductions in astrocyte number and associated morphological changes observed in depression, including decreased occupied area and degree of ramification (15–19).

In addition, SSRIs modulate intracellular signalling pathways in astrocytes. Antidepressants have been shown to potentiate astrocytic cyclic adenosine monophosphate (cAMP) signalling by elevating intracellular cAMP levels and promoting the activation of cAMP response element-binding protein (CREB) (20). cAMP is an ubiquitous second messenger in the central nervous system, generated from adenosine triphosphate (ATP) by adenylate cyclase, and both cAMP levels and adenylate cyclase expression have been extensively studied in the context of depression (21). Expression of adenylate cyclase 2, one of ten adenylate cycle isoforms, is decreased in a mouse model of anxiety and also dysregulated in patients with depression (22,23). Some studies suggest that astrocytic cAMP-dependent signalling may contribute to SSRI-induced synaptic plasticity, in part through increased expression of brain-derived neurotrophic factor (BDNF) (24–27). However, the mechanisms by which antidepressants such as SSRIs potentiate cAMP signalling in astrocytes remain incompletely understood. One potential pathway under discussion is the SSRI-induced relocation of Gαs from lipid raft domains to non-raft regions of the plasma membrane, thereby facilitating activation of cAMP signalling pathways (24,28,29).

Another study suggested that antidepressant-induced activation of the cAMP-CREB pathway requires P2Y11 and adenosine 2B (A2B) receptors, and ATP release dependent on the vesicular

bioRxiv preprint doi: https://doi.org/10.64898/2026.06.04.730071; this version posted June 8, 2026. The copyright holder for this preprint (which was not certified by peer review) is the author/funder, who has granted bioRxiv a license to display the preprint in perpetuity. It is made available under a CC-BY 4.0 International license.

nucleotide transporter (VNUT) (30). Genetic deletion of VNUT selectively in astrocytes markedly attenuated both fluoxetine-induced ATP release and antidepressant-like behavioural effects, establishing a causal link between astrocytic purinergic signalling and therapeutic efficacy (30). However, FLX targets mediating ATP release from astrocytes and signalling events linking ATP release to cAMP elevation in astrocytes are unknown.

In this study, we show that FLX-driven elevation of cAMP in astrocytes requires microglia-astrocyte crosstalk and is mediated by purinergic signalling. Specifically, we discovered that SSRI FLX engages astrocytic 5-HT2B receptors for ATP release. Extracellular ATP then is converted by microglia to adenosine, which, in turn, acts on astrocytic Gs-coupled A2B receptors, resulting in elevated astrocytic cAMP.

Methods

Primary glial cell culture

All procedures complied with the UK Home Office (Scientific Procedures) Act (1986) and were approved by the University of Bristol ethical committee (UIN25050). Primary astrocytes were prepared as described previously (31). Briefly, Wistar Han IGS female and male rat pups at postnatal days 3-8 were culled using schedule 1 method, and midbrain tissue was immediately dissected and dissociated in HBSS (Gibco, 14175129) containing 3 mg/mL BSA (Sigma-Aldrich, A3294), 0.04 mg/mL DNase I (Merck, D5025), and 0.025 mg/mL trypsin (Sigma-Aldrich, T9935). Cells were maintained in T75 flasks in DMEM GlutaMAX (Gibco, 61965059) supplemented with 10% FBS (heat inactivated, Gibco, 12483020) and 1% penicillin-streptomycin (Sigma-Aldrich, P4333) at 37 °C and 5% CO_2.

Primary astrocytes were treated with 10μM of FLX, a dose chosen from human studies showing that at a clinically low dose of FLX (20mg/kg) its concentrations in the brain reaches 10 to 30μM

bioRxiv preprint doi: https://doi.org/10.64898/2026.06.04.730071; this version posted June 8, 2026. The copyright holder for this preprint (which was not certified by peer review) is the author/funder, who has granted bioRxiv a license to display the preprint in perpetuity. It is made available under a CC-BY 4.0 International license.

throughout a course of treatment (32) while higher clinically relevant doses result in FLX concentrations up to 50μM in the human brain (33,34). Previously reported and our own preliminary cell culture experiments (Supplementary Table 1) confirmed that this dose does not affect astrocyte survival (35,36).

Viral transduction and live-cell imaging

Astrocytes were plated on collagen-coated glass coverslips (2×10^5 cells/mL, 24-well plates) and transduced at seeding with adenoviral vectors (AVV) encoding sensors (MOI 50-100): AVV-mCMV/GfaABC1D-Epac-S^{H187} (FRET; cAMP; gift from Kees Jalink and Anne Lann) (37), AVV-mCMV/GfaABC1D-Twitch2B (FRET; Ca^{2+}; gift from Oliver Griesbeck) (38), and AVV-CMV-GRAB-ATP1.0 (GRAB-ATP1.0; gift from Yulong Li, Addgene plasmid #167582; http://n2t.net/addgene:167582; RRID:Addgene_167582) (39). Imaging was performed after 2-4 days post-transduction.

Time-lapse imaging was conducted on a Leica SP5 confocal microscope (40× water objective) in a temperature controlled chamber with continuous superfusion of HEPES-buffered saline (pH 7.4) at 2.5ml/min for imaging of FRET sensors or 5ml/min for imaging of GRAB-ATP1.0 sensor. Drugs were delivered by bath. Images were acquired every 2s (GRAB-ATP1.0) or 5 s (FRET) for 1200 s (512 × 512 pixels). FRET sensors were excited by 458 nm Ar laser line; emissions were collected at 465–500 nm (donor) and 515–595 nm (acceptor). Excitation for both the GRAB-ATP1.0 sensor was 488nm, and emissions were collected at 500-600nm. Regions of interest were analysed in LAS X and exported for processing in R. Signals were normalised to baseline of 180s or 300 s and specified in figure legends.

Determination of ATP release

ATP release was quantified using the RealTime-Glo Extracellular ATP Assay (Promega, GA5010). Astrocytes (6×10^4 cells/well) were plated in opaque 96-well plates, equilibrated in HBSS with 7

bioRxiv preprint doi: https://doi.org/10.64898/2026.06.04.730071; this version posted June 8, 2026. The copyright holder for this preprint (which was not certified by peer review) is the author/funder, who has granted bioRxiv a license to display the preprint in perpetuity. It is made available under a CC-BY 4.0 International license.

mM glucose and treatments, and luminescence was recorded kinetically at 37 °C using a Tecan plate reader (TECAN, infiniteM200pro). Background was subtracted, and values normalised to controls.

Depletion of microglia

Microglia were depleted using the CSF1R inhibitor PLX5622 (10 μM, 7-10 days; medium refreshed every 3 days). Cultures were maintained in PLX-supplemented media prior to experiments, and depletion was verified by loss of microglial marker ionised calcium-binding adaptor molecule 1 (Iba-1).

Immunohistochemistry

Coverslips seeded with glia culture 24 hours prior ($2x10^5$ cells/ml) were fixed with 4% paraformaldehyde solution (15 min, room temperature (RT)) and then washed with PBS. Cells were permeabilised in blocking solution (10% FBS and 0.3% Triton-X100 in PBS; 30 mins, RT) and then incubated with primary antibodies against astrocyte-specific glial fibrillary acidic protein (GFAP) (anti-GFAP, rabbit, Dako, GA524, 1:500) or microglia-specific Iba1 (anti-Iba1, guinea pig, Synaptic Systems/234 308, 1:400) in an antibody solution (3% FBS and 0.1% Triton-X100 in PBS) at 4°C for 16 hours. After PBS washes to remove excess primary antibodies, cells were incubated with secondary antibodies, goat anti-rabbit Alexa Fluor 488 (Invitrogen, R37116, 2 drops/ml) or goat anti-guinea pig Alexa Fluor 594 (Invitrogen, A11076, 1:500). Coverslips were air-dried and mounted on slides using FluorSave mounting media (Millipore, 345789). Stained coverslips were imaged using a 20x air objective on a Leica SP5 confocal microscope.

Statistical analysis

For analysis of data generated using FRET sensors, the FRET ratio was calculated and normalised to the baseline of each recording across all presented data, except in Figure 4D, where non-normalised values are reported. Normalised FRET ratio were calculated using a

bioRxiv preprint doi: https://doi.org/10.64898/2026.06.04.730071; this version posted June 8, 2026. The copyright holder for this preprint (which was not certified by peer review) is the author/funder, who has granted bioRxiv a license to display the preprint in perpetuity. It is made available under a CC-BY 4.0 International license.

custom-made R script (V4.1.1). Next, each recording was carefully assessed to ensure that the baseline was stable, and focus was consistent throughout the recording. For both FRET sensor and GRAB-ATP1.0 recordings, the area under the curve (AUC) was calculated from 300 to 1200 seconds using GraphPad Prism (V11).

For all experiments, to determine if the drug(s) tested changed the tested parameter, a one-sample t-test from zero was used. To assess the significance between experimental groups, an unpaired t-test was used for two groups and a one-way analysis of variance (ANOVA) with, if necessary, a post-hoc Holm-Šídák test was used for comparing more than two groups.

Results

FLX elevates intracellular cAMP levels without affecting Ca^{2+} dynamics in primary rat astrocytes

Intracellular levels of Ca^{2+} and cAMP following FLX application (10µM, 5 minutes) were quantified using live-cell confocal imaging of Twitch2B and Epac-S^{H187} FRET sensors, respectively, in rat primary astrocytes (Figure 1A&B). FLX had no effect on intracellular Ca^{2+} levels ($t(22)=1.487$, $p=0.1511$, Figure 1B&C), in contrast to ATP (10µM, 5 minutes) which triggered a robust elevation by 160% compared to baseline ($t(19)=8.311$, $p<0.0001$), verifying that the sensor accurately reports Ca^{2+} changes (Figure 1B&C).

FLX application elevated astrocytic cAMP levels by 28% compared to baseline (mean AUC: 27.98±26.70; $t(16)=4.320$, $p=0.0005$, Figure 1E&F).

Co-application of FLX with the AC inhibitor NKY80 (NKY; 10µM; 17 minutes) blocked FLX-evoked cAMP increase (NKY+FLX vs zero: ($t(24)=0.9299$, $p=0.3617$, or vs. FLX: $p=0.0044$, Figure 1E&F). In comparison, the AC activator, NKH477 (NKH; 3µM, 3 minutes) increased intracellular cAMP in astrocytes by 164% (mean AUC: 163.5±129.2; $t(22)=6.067$, $p<0.0001$, Figure 1G), which was

bioRxiv preprint doi: https://doi.org/10.64898/2026.06.04.730071; this version posted June 8, 2026. The copyright holder for this preprint (which was not certified by peer review) is the author/funder, who has granted bioRxiv a license to display the preprint in perpetuity. It is made available under a CC-BY 4.0 International license.

attenuated by NKY80 (NKY vs zero: (t(12)=4.361, p=0.009, vs. NKH: t(34)=3.518, p=0.0013, Figure 1G).

FLX-driven increase in astrocytic cAMP requires both the A2B and 5-HT2B receptors

To delineate the signalling mechanisms underlying the FLX-induced increase in intracellular cAMP in astrocytes, we examined the potential involvement of receptors previously implicated in the regulation of astrocytic cAMP levels or to which FLX was reported to have affinity.

First, we tested A2B receptor involvement in FLX-triggered cAMP signalling in astrocytes. Functional expression of the A2B receptor has been demonstrated in astrocytes both *in vivo* and *in vitro* in previous studies (40,41), and was also confirmed in our astrocyte cultures (Supplementary Table 2). As the A2B receptor is Gs-coupled, it would be expected to lead to an increase in intracellular cAMP levels if FLX were to engage it.

FLX-triggered increase in astrocytic cAMP was blocked by a highly selective antagonist of A2B receptor (PSB603 (PSB); 10μM; FLX+PSB vs. zero: t(28)=0.4130, p=0.6828; vs. FLX: p<0.0001; Figure 2A&B). We confirmed that PSB is able to block A2B-driven cAMP elevation (PSB+adenosine vs. zero: t(17)=0.6917, p=0.4985; vs. ADO: p=0.0029;) as a response to its intrinsic ligand adenosine (by 113%; adenosine vs. zero: t(49)=8.889, p<0.000110μM; Figure 2D).

Notably, the temporal dynamics of cAMP responses differ between adenosine and FLX. FLX requires significantly longer time to reach the maximal response compared to adenosine (mean time (s) ± SD: ADO = 657.2±129.4s; FLX = 906.2±340.9s; t(31)=2.739, p=0.0101), indicating that FLX-stimulated increase in cAMP is indirect, and suggesting that FLX engages another target upstream of the A2B receptor. We therefore tested whether the 5-HT2B receptor, to which FLX has high affinity, could contribute to the fluoxetine-induced cAMP elevation in astrocytes. This is feasible since 5-HT2B receptor expression has been found in murine astrocytic cultures (42)

bioRxiv preprint doi: https://doi.org/10.64898/2026.06.04.730071; this version posted June 8, 2026. The copyright holder for this preprint (which was not certified by peer review) is the author/funder, who has granted bioRxiv a license to display the preprint in perpetuity. It is made available under a CC-BY 4.0 International license.

and human astrocytes (43), and in our rat astrocyte cultures (Supplementary Table 2 and 3; Supplementary Figure 1).

FLX-induced increase in astrocytic cAMP was abolished by a specific 5-HT2B receptor antagonist LY266097 (LY; 10μM; LY vs. zero: $t(17)=0.6917$, $p=0.4985$; vs. FLX: $p=0.0029$, Figure 2B&C). While application of 5-HT2B receptor agonist BW-723C86 (BW; 1μM; 5 minutes) significantly elevated intracellular astrocytic cAMP by 40% ($t(22)=11.760$, $p<0.0001$) and to an extent comparable to that induced by FLX ($t(37)=2.007$, $p=0.0521$; Figure 2B&C).

Altogether these data indicate that FLX-induced elevation of cAMP in astrocytes requires coordinated engagement of two receptor systems, with A2B receptor activation occurring downstream of 5-HT2B receptor signalling (Figure 2E). We hypothesised that stimulation of the 5-HT2B receptor results in autocrine activation of A2B receptors by adenosine. It is well established that a significant proportion of extracellular adenosine comes from conversion of ATP by extracellular nucleases (44). Therefore, we next investigated whether FLX can evoke ATP release from astrocytes.

FLX engages 5-HT2B receptors to trigger ATP release in primary rat astrocytes

To quantify extracellular ATP dynamics following FLX treatment, we first employed the genetically encoded fluorescent sensor GRAB-ATP1.0. FLX application produced a significant increase in extracellular ATP levels by 10% ($t(28)=2.111$, $p=0.0438$; Figure 3A). However, given the rapid kinetics and spatial complexity of ATP signalling, as well as the continuous basal release of ATP by astrocytes, which can further propagate ATP release in neighbouring cells (43), it was challenging to reliably quantify ATP dynamics following pharmacological treatments using GRAB-ATP1.0. We therefore complemented these experiments with a real-time ATP luminescence assay to independently validate the findings. Consistent with the extracellular sensor data, FLX treatment significantly increased ATP release relative to control by 2% (FLX vs. control $p=0.0082$; Figure 3B&C). Given complexity of astrocyte ATP signalling combined with the

bioRxiv preprint doi: https://doi.org/10.64898/2026.06.04.730071; this version posted June 8, 2026. The copyright holder for this preprint (which was not certified by peer review) is the author/funder, who has granted bioRxiv a license to display the preprint in perpetuity. It is made available under a CC-BY 4.0 International license.

large assay volume (100µl), accurately measuring short-term local ATP dynamics is technically challenging using luminescent detection. Although we managed to achieve reliable and reproducible results on ATP release using luminescent assay, which allowed us to test various pharmacological agents, the observed responses were modest and likely do not reflect local intercellular ATP fluctuations.

Inhibition of 5-HT2B receptors with the selective antagonist LY effectively blocked the FLX-induced increase in ATP release. (LY+FLX vs FLX: $p<0.0001$; Figure 3B&C), demonstrating that this effect is dependent on 5-HT2B receptor activation. Collectively, these data support a model in which FLX engages 5-HT2BR to stimulate ATP release, which in turn acts in an autocrine manner to drive A2B receptor-dependent cAMP production in astrocytes. However, because ATP does not directly bind to the A2B receptor, we next examined whether extracellular ATP is metabolized to adenosine, which could subsequently activate A2B receptor signalling.

FLX increases astrocytic cAMP by engaging microglia and purinergic signalling

Our rat primary astrocyte cultures were prepared using a standard protocol to minimise microglial contamination (31). However, a residual amount of microglia is still detected in our primary astrocyte preparation (Figure 4A). Microglia play an important role in converting extracellular ATP to adenosine since they are the main cellular source of CD39, which catalyses the first step in that process (45) (Figure 4F). To assess the contribution of microglia to FLX-driven signalling, we treated astrocyte cultures with a microglia-specific CSF1R inhibitor PLX5622 to ablate microglia (45). Indeed, 7-day treatment with PLX5622 (10µM) resulted in near-complete microglial depletion with only an occasional microglial cell detected in the whole field of view (PLX5622-treated vs untreated primary rat astrocyte cultures, $p<0.0001$; Figure 4A&B).

FLX-induced elevations in astrocytic cAMP were reduced by 62% following microglial depletion ($t(38)=2.645$, $p=0.0118$, Figure 4C). However, microglia depletion did not completely abolish

bioRxiv preprint doi: https://doi.org/10.64898/2026.06.04.730071; this version posted June 8, 2026. The copyright holder for this preprint (which was not certified by peer review) is the author/funder, who has granted bioRxiv a license to display the preprint in perpetuity. It is made available under a CC-BY 4.0 International license.

FLX-triggered increase in astrocytic cAMP, as there still was a significant increase by 15% in cAMP levels in PLX5622-treated cultures in response to FLX ($p<0.0001$, Figure 4C).

If microglia substantially contribute to the conversion of extracellular ATP to adenosine, microglial ablation should lead to an accumulation of ATP in response to FLX treatment. Indeed, in PLX5622-treated primary astrocyte cultures, ATP release is 60% higher than in untreated cultures ($t(5.906)=9.149$, $p=0.001$, Figure 4D).

Similarly, if microglia plays a major role in ATP-to-adenosine conversion within our experimental system, exogenous ATP conversion into adenosine should be suppressed by microglial ablation, thereby diminishing A2B receptor-dependent cAMP elevation. Indeed, ATP-triggered increase in astrocyte cAMP is reduced by 55% in microglia-depleted cultures compared to astrocytes from regular cultures ($t(101.9)=9.605$, $p<0.0001$, Figure 4E).

Together, these findings indicate that microglia plays a critical intermediary role in the ATP-to-adenosine axis underlying FLX-induced cAMP signalling. Specifically, they support a model in which FLX stimulates ATP release from astrocytes, which is subsequently metabolised with the aid of microglia into adenosine, thereby amplifying A2B receptor-dependent cAMP production.

Discussion

Accumulating evidence highlights astrocytic signalling as a critical component of the antidepressant actions of monoaminergic drugs. SSRIs have been shown to activate astrocytic cAMP signalling, a pathway typically reduced in depression and restored by antidepressant treatment, thereby contributing to their therapeutic efficacy. Yet, the mechanisms underlying antidepressant-induced modulation of astrocytic cAMP remain insufficiently understood. Here, we identify a novel mechanism driving astrocytic cAMP levels following FLX treatment which

bioRxiv preprint doi: https://doi.org/10.64898/2026.06.04.730071; this version posted June 8, 2026. The copyright holder for this preprint (which was not certified by peer review) is the author/funder, who has granted bioRxiv a license to display the preprint in perpetuity. It is made available under a CC-BY 4.0 International license.

involves astrocyte-to-microglia crosstalk and purinergic signalling, providing a mechanistic framework for understanding how antidepressants regulate astrocyte function.

Specifically, we show that FLX promotes ATP release in a process dependent on astrocytic 5-HT2B receptors. Microglia, being the main cellular source of CD39, subsequently contribute to the conversion of FLX-induced extracellular ATP into adenosine, which then acts on astrocytic A2B receptors, increasing in intracellular cAMP levels (Figure 4F).

5-HT2B receptors are required for the observed increase in astrocytic cAMP levels. However, we did not detect a concomitant rise in intracellular Ca^{2+}, despite their canonical classification as Gq-coupled GPCRs (46). However, the literature indicates that their signalling repertoire is considerably broader and highly context dependent. In addition to classical PLC/IP3/Ca^{2+} signalling, 5-HT2B receptors have been shown to engage ERK/MAPK, PI3K/Akt, β-arrestin-dependent, and receptor-transactivation pathways in a cell type- and ligand-specific manner (47–50). 5-HT2B receptor agonist, BW723C86, has been reported to be unable to evoke Ca^{2+} levels in brainstem astrocytes (51). Consistent with this signalling plasticity, we found that 5-HT2B receptor engagement was required for the fluoxetine-induced increase in astrocytic cAMP despite the absence of a detectable Ca^{2+} rise, indicating that, in our preparation, 5-HT2B receptors are functionally coupled to a non-canonical signalling pathway. Activation of 5-HT2B receptors with the selective agonist BW723C86 produced a significant although indirect response on intracellular cAMP, further demonstrating that 5-HT2B is functional in our preparation and its signalling extends beyond classical Gq coupling. Together, these data establish that fluoxetine increases astrocytic cAMP via a Ca^{2+}-independent mechanism, indicating that Ca^{2+} mobilisation is not required for this component of antidepressant action.

The 5-HT2B receptor is expressed by astrocytes throughout the mouse brain. Comparing expression between the striatum, hippocampus and cortex, 5-HT2B receptor is expressed the highest in the striatum, with the lowest expression in the cortex. Relative to GFAP, 5-HT2B

bioRxiv preprint doi: https://doi.org/10.64898/2026.06.04.730071; this version posted June 8, 2026. The copyright holder for this preprint (which was not certified by peer review) is the author/funder, who has granted bioRxiv a license to display the preprint in perpetuity. It is made available under a CC-BY 4.0 International license.

receptor expression is around 7-fold lower in the striatum and 9-fold less in the hippocampus (40). In humans, according to the Human Protein Atlas, microglial 5-HT2B receptor expression is double that of astrocytes (52,53). However, in cultures, 5-HT2B receptor expression is higher in astrocytes than in both microglia and neurons (54).

Here, we show that FLX requires 5-HT2B receptor to stimulate ATP release from astrocyte. SSRIs were previously reported to facilitate ATP release specifically from astrocytes via VNUT (30,55) or gap junctions (56). Preclinically, interfering with mechanisms of ATP release induces a depressive-like phenotype that can be reversed by ATP administration, and maintaining ATP levels in the mPFC are also crucial for regulating depressive-like behaviour (57,58). Hertz et al., (2015), demonstrated that FLX engages 5-HT2B receptor to regulate intracellular pathways in astrocytes (59), while other published studies revealed lack of 5-HT2B receptor compromises therapeutic effects of FLX (13,14).

Ectonucleotidases CD39 and CD73 represent the principal enzymatic pathway mediating the extracellular conversion of ATP to adenosine (44). Both enzymes exist in membrane-bound forms and as soluble or extracellular vesicle-associated variants within the extracellular milieu (60,61). Expression patterns are cell-type specific, with CD73 most abundantly expressed in neurons and relatively low levels observed in astrocytes, whereas CD39 is markedly enriched in microglia, with expression reported to be 20 times higher than in astrocytes (45). Therefore, particularly in glial cultures, microglia may play a predominant role in adenosine generation from ATP. Although astrocytes predominate in our cultures, low levels of Iba1 are still detectable (Figure 4; Supplementary Table 2).

Indeed, here we showed that in PLX5622-treated cultures, there is a significant reduction in FLX- and ATP-driven increases in cAMP. While unstimulated ATP release was elevated in PLX5622-treated cultures compared with controls, consistent with impaired ATP catabolism in the

bioRxiv preprint doi: https://doi.org/10.64898/2026.06.04.730071; this version posted June 8, 2026. The copyright holder for this preprint (which was not certified by peer review) is the author/funder, who has granted bioRxiv a license to display the preprint in perpetuity. It is made available under a CC-BY 4.0 International license.

absence of microglia and supporting a critical role for microglia in converting extracellular ATP to adenosine.

Microglia contribution to FLX-driven cAMP elevation in astrocytes could go beyond ATP-to-adenosine conversion. It is possible that the 5-HT2B receptor, expressed in both cell types, potentiates ATP release from both astrocytes and microglia following FLX treatment. Furthermore, it has been demonstrated that astrocytic ATP release stimulates microglial ATP release (55).

Expression of the A2B receptor in murine astrocytes varies across brain regions, with the highest expression found in the hippocampus. Relative to GFAP, A2B receptor expression levels are about 4-fold lower in the striatum, 5-fold lower in the hippocampus and 1-fold lower in the cortex (40). In humans, A2B receptor expression is 25 times higher in astrocytes than in both neurons and microglia (52,53). Our data demonstrate that cAMP elevations are a consequence of activation of the A2B receptors following potentiated release of ATP as a result of 5-HT2B receptor activation. Although microglial depletion attenuated the FLX-induced cAMP increase, it did not completely abolish it, suggesting a minor astrocytic contribution to ATP-to-adenosine conversion. Another possibility is that FLX directly promotes adenosine release from astrocytes, a phenomenon observed in astrocytes following ketamine treatment (62).

Our data indicate a mechanism by which alterations to cAMP signalling in depression can be restored. Antidepressants have been reported to potentiate astrocytic cAMP signalling by increasing intracellular cAMP levels and activating CREB (20). Further, expression of adenylate cyclase 2 is decreased in both animal models of anxiety and patients with depression (22,23). Enhanced astrocytic cAMP signalling may also contribute to antidepressant-induced synaptic plasticity, in part by increasing BDNF expression (24–27). Our data provides a mechanism by which FLX restores cAMP levels in astrocytes, identifying a pathway by which antidepressants may recover depressive symptoms. Given the central role of cAMP signalling in regulating

bioRxiv preprint doi: https://doi.org/10.64898/2026.06.04.730071; this version posted June 8, 2026. The copyright holder for this preprint (which was not certified by peer review) is the author/funder, who has granted bioRxiv a license to display the preprint in perpetuity. It is made available under a CC-BY 4.0 International license.

astrocyte function and morphology, elevations in cAMP may represent a mechanism through which antidepressant treatment restores astrocytic structure and homeostasis (15,17,19).

We tested a single FLX concentration of 10 μM. This dose was selected because it falls within the range of fluoxetine concentrations reported in the human brain during therapeutic treatment, estimated across studies at approximately 0.3-42 μM (32,63,64). Depending on clinical dose, brain concentrations range from 10-30μM following a treatment of a clinically low dose (20mg/kg), and up to 50μM following higher, clinically relevant doses (120mg/kg) (32–34). Thus, 10 μM represents a physiologically relevant concentration that is also commonly used in experimental models. In addition, previous studies and our own preliminary cell culture experiments indicated that this concentration does not compromise astrocyte viability (35,36). Finally, the reported Ki of the 5-HT2B receptor for FLX is greater than 10 μM, although this remains an area of an ongoing debate (59,65,66).

There is a large volume of literature surrounding the mechanistic properties of antidepressants and the pathophysiology of depression (8). In this study, we demonstrate a mechanism by which FLX alters the signalling dynamics of glia, principally astrocytes. It is clear that the mechanisms of action of antidepressants are complex; in this study, we do not discount any other mechanisms of action of depression, and propose that antidepressants act on multiple pathways simultaneously. Here, we not only identify a pathway through which FLX modulates glial signalling, but also provide support for several proposed mechanisms underlying antidepressant action. First, our findings confirm the involvement of the 5-HT2B receptor, which has been suggested to be an important mediator of antidepressant effects (13,14,42). Second, the participation of microglia is consistent with growing evidence implicating these cells in both the pathophysiology of depression and the mechanisms of antidepressant response (67–70). Our data support previous reports that FLX potentiates ATP release, further aligning with evidence that ATP itself may exert antidepressant-like effects (30,56–58). Finally, our data

bioRxiv preprint doi: https://doi.org/10.64898/2026.06.04.730071; this version posted June 8, 2026. The copyright holder for this preprint (which was not certified by peer review) is the author/funder, who has granted bioRxiv a license to display the preprint in perpetuity. It is made available under a CC-BY 4.0 International license.

support the evidence that cAMP signalling is implicated in depression, and the mechanism of action of antidepressants (20,22,23).

While our data focuses on acute signalling events, prior work indicates that chronic antidepressant administration modulates glial purinergic pathways and downstream effectors, including adenosine receptor-linked cAMP pathways, which may contribute to longer-term neuroplastic and behavioural effects of SSRIs beyond immediate second-messenger changes (30).

In summary, our findings identify a previously unrecognised glial mechanism through which fluoxetine modulates astrocyte signalling. We show that FLX engages the 5-HT2B receptor to promote ATP release, after which microglia facilitate the extracellular conversion of ATP to adenosine, leading to activation of astrocytic A2B receptors and elevation of intracellular cAMP. This pathway provides a mechanistic explanation for the long-observed ability of antidepressants to enhance astrocytic cAMP/CREB signalling and supports growing evidence that astrocytes, microglia, purinergic signalling, and cAMP-dependent plasticity are central to antidepressant responses. More broadly, these data reinforce the view that SSRIs act not only through neuronal monoamine systems, but also by reshaping cooperative glial signalling networks that may underlie therapeutic recovery.

bioRxiv preprint doi: https://doi.org/10.64898/2026.06.04.730071; this version posted June 8, 2026. The copyright holder for this preprint (which was not certified by peer review) is the author/funder, who has granted bioRxiv a license to display the preprint in perpetuity. It is made available under a CC-BY 4.0 International license.

Figure legends

Figure 1: Fluoxetine enhances astrocytic cAMP signalling.

(A) Representative image of primary rat astrocytes transduced with adenoviral vectors (AVVs) to express intracellular calcium FRET sensor Twitch2B (AVV-mCMV/GfaABC1D-Twitch2B). Average traces **(B)** and summary data **(C)** illustrating changes in intracellular calcium levels ($[Ca^{2+}]_i$; Twitch2B; fluorescence intensity (FI) ratio of cpVenus:mCeruleuan3) in primary rat astrocytes following application of fluoxetine (FLX, 10µM, 5mins) or ATP (1µM, 5mins). **(D)** Representative image of primary rat astrocytes transduced with AVVs to express intracellular cAMP sensor Epac-S^{H187} (AVV-sGFAP-cAMPhigh^{H187}). Average traces **(E)** and summary data **(F)** illustrating changes in intracellular cAMP levels ($[cAMP]_i$; Epac-S^{H187}; FI ratio of mTurquoise2:Venus) in primary rat astrocytes following application of FLX (10µM, 5mins) along or in combination with adenylate cyclase inhibitor NKY80 (NKY, 10µM; NKY 180-1200s and FLX 300-480s), or NKY alone (10µM; 180-1200s). **(G)** Summary data illustrating changes to $[cAMP]_i$ following application of adenylate cyclase activator NKH477 (NKH, 3µM, 300-480s) alone or in combination with adenylate cyclase inhibitor NKY80 (NKY, 10µM; NKY 180-1200s and NKH 300-480s). Scale bar = 50µm.

Data are presented as mean ± standard deviation with each data point representing a region of interest (ROI). The numbers in parentheses indicate the number of individual ROIs and separate cultures (animals). $^{\#\#\#\#}p<0.0001$, $^{\#\#\#}p<0.001$ vs zero, one sample t-test; $^{**}p<0.01$, $^{*}p<0.05$ vs FLX, $^{\$\$}p<0.01$ vs NKH; unpaired t-test (C and G) or one-way ANOVA with post-hoc Holm-Šídák's test (F).

Figure 2: The fluoxetine-triggered increase in astrocytic cAMP requires both adenosine A2B and serotonin 5-HT2B receptors.

bioRxiv preprint doi: https://doi.org/10.64898/2026.06.04.730071; this version posted June 8, 2026. The copyright holder for this preprint (which was not certified by peer review) is the author/funder, who has granted bioRxiv a license to display the preprint in perpetuity. It is made available under a CC-BY 4.0 International license.

Average traces **(A)** illustrating changes in intracellular cAMP levels (Epac-S^{H187}; fluorescence intensity (FI) ratio) in primary rat astrocytes following application of FLX (10μM, 5mins), or in combination with adenosine 2B (A2B) receptor antagonist PSB603 (PSB, 10μM, 300-1200s). Summary data **(B)** illustrating changes to $[cAMP]_i$ following application of FLX, BW, PSB, FLX+PSB, LY, and LY+FLX. Average traces **(C)** illustrating changes to $[cAMP]_i$ following application of FLX alone, or in combination with serotonin 2B receptor ($5\text{-}HT_{2B}R$) antagonist LY266097 (LY, 10uM, 300-1200s) or $5\text{-}HT_{2B}R$ agonist BW723C86 (BW,1μM, 5mins). **(D)** Summary data illustrating changes to $[cAMP]_i$ following application of adenosine (ADO, 10μM, 480-600s) alone or in combination with $A_{2B}R$ antagonist (PSB, 10μM, 300-1200s). **(E)** Schematic illustration of signalling pathways involved in FLX-driven recruitment of astrocytic cAMP: AC – adenylate cyclase; round arrow – agonist; flat arrow – antagonist.

Data are presented as mean ± standard deviation with each data point representing a region of interest (ROI). The numbers in parentheses indicate the number of individual ROIs and separate cultures (animals). $^{\#\#\#\#}p<0.0001$ vs zero, one sample t-test; $^{****}p<0.0001$, $^{**}p<0.001$, $^{*}p<0.01$ vs FLX, $^{\$\$\$\$}p<0.0001$, $^{\$\$}p<0.001$ vs BW (C), one-way ANOVA with post-hoc Holm-Šídák's test; $^{\$\$\$\$}p<0.0001$ vs ADO (D), unpaired t-test (D).

bioRxiv preprint doi: https://doi.org/10.64898/2026.06.04.730071; this version posted June 8, 2026. The copyright holder for this preprint (which was not certified by peer review) is the author/funder, who has granted bioRxiv a license to display the preprint in perpetuity. It is made available under a CC-BY 4.0 International license.

Figure 3: Fluoxetine potentiates astrocytic ATP release via serotonin 2B receptor.

(A) Amount of ATP released by primary rat astrocytes transduced with AVVs to express extracellular GRAB-ATP1.0 sensor (AVV-CMV-GRAB-ATP1.0) following application of fluoxetine (FLX, 10µM, 300-600s) or HBS as control (Ctr). Average traces **(B)** and summary data **(C)** illustrating changes in extracellular ATP levels following application of FLX (10µM, 4 hours) along or serotonin 2B receptor antagonist LY266097 (LY, 10µM, 5 hrs) or combination of both (LY for 1hr then LY+FLX for 4hrs).

Data are presented as mean ± standard deviation with each data point representing a region of interest (ROI; A) or a well (B and C). The numbers in parentheses indicate the number of individual ROIs (A) or well (B and C) and separate cultures (animals). $^{\#\#\#\#}$p<0.0001, $^{\#\#}$p<0.01, $^{\#}$p<0.05 vs control, ****p<0.0001, **p<0.01, *p<0.05 vs FLX, $^{\$\$}$p<0.01 vs LY, paired t-test (A) or one-way ANOVA with post-hoc Holm-Šídák's test (C).

Figure 4: Fluoxetine-driven increase in astrocytic cAMP signaling requires microglia-astrocyte crosstalk mediated by purinergic signaling.

Successful microglial depletion by an inhibitor of microglia-specific colony-stimulating factor 1 receptor (PLX5622, PLX, 10µM, 7 days): **(A)** Representative images of staining against astrocyte-specific glial fibrillary acidic protein (GFAP) and microglia-specific ionised calcium-binding adapter molecule 1 (Iba1) and **(B)** quantification of Iba1-positive cells in culture. Scale bar = 20µm. **(C)** Summary data illustrating changes in cAMP levels (Epac-S^{H187}; fluorescence intensity (FI) ratio) in primary rat astrocytes with or without PLX treatment following application of fluoxetine (FLX 10µM, 5mins). **(D)** Summary data illustrating changes in extracellular ATP levels in rat astrocyte cultures treated with PLX. **(E)** Summary data illustrating changes in cAMP levels (Epac-S^{H187}; fluorescence intensity (FI) ratio) in primary rat astrocytes with or without PLX treatment following application of adenosine triphosphate (ATP, 50µM, 3mins). **(F)** Schematic

bioRxiv preprint doi: https://doi.org/10.64898/2026.06.04.730071; this version posted June 8, 2026. The copyright holder for this preprint (which was not certified by peer review) is the author/funder, who has granted bioRxiv a license to display the preprint in perpetuity. It is made available under a CC-BY 4.0 International license.

illustration of signalling pathways involved in FLX-driven recruitment of astrocytic cAMP: Pointed arrow - potentiated; flat arrow - antagonist; rounded arrow - agonist; cross arrow - inhibition; $A_{2B}R$: adenosine 2B receptor; 5-HT2BR – serotonin 2B receptor; AC: adenylate cyclase.

Data are presented as mean ± standard deviation, with each data point representing a field of view (B) or region of interest (C and D) (ROI) or well (E). The numbers in parentheses indicate the number of individual field of view (b) or ROI (C and D) or well (E), and separate cultures (animals). $^{\$\$\$\$}p<0.0001$, $^{\$\$\$}p<0.001$, $^{\$}p<0.05$ vs PLX-free culture, Mann-Whitney test (B), or unpaired t-test (C-E), $^{\#\#\#}<0.001$, $^{\#\#}<0.01$ one-sample t-test from 0 (C).

bioRxiv preprint doi: https://doi.org/10.64898/2026.06.04.730071; this version posted June 8, 2026. The copyright holder for this preprint (which was not certified by peer review) is the author/funder, who has granted bioRxiv a license to display the preprint in perpetuity. It is made available under a CC-BY 4.0 International license.

Acknowledgements

The study was supported by the AMS Springboard award SBF005\1102 and the MRC Career Development Award MR/T031115/1 to VM.

We would like to thank Dr Stephen J Chuter for his assistance in generating the R scripts for analysis. We thank K. Jalink and A. Lann for providing the Epac-SH187 sensor clones, and O Griesbeck for donating the Twitch2B sensor clones.

Code availability

The code used to calculate FRET ratio and normalised FRET ratio is available from the GitHub repository: https://github.com/marstoncatriona/FRETSensorAnalysis.

bioRxiv preprint doi: https://doi.org/10.64898/2026.06.04.730071; this version posted June 8, 2026. The copyright holder for this preprint (which was not certified by peer review) is the author/funder, who has granted bioRxiv a license to display the preprint in perpetuity. It is made available under a CC-BY 4.0 International license.

References

1. Organisation TWH. Depression Fact Sheet [Internet]. 2021 [cited 2021 Oct 7]. Available from: https://www.who.int/news-room/fact-sheets/detail/depression

2. IQVIA. The Global Use of Medicines Outlook Through 2029 [Internet]. [cited 2026 Mar 18]. Available from: https://www.iqvia.com/insights/the-iqvia-institute/reports-and-publications/reports/the-global-use-of-medicines-outlook-through-2029

3. Medicines used in mental health – England – 2015/16 to 2024/25 | NHSBSA [Internet]. [cited 2026 Mar 9]. Available from: https://www.nhsbsa.nhs.uk/statistical-collections/medicines-used-mental-health-england/medicines-used-mental-health-england-201516-202425

4. Saelens J, Gramser A, Watzal V, Zarate CA, Lanzenberger R, Kraus C. Relative effectiveness of antidepressant treatments in treatment-resistant depression: a systematic review and network meta-analysis of randomized controlled trials. Neuropsychopharmacol. 2025 May;50(6):913–9. doi:10.1038/s41386-024-02044-5

5. Cipriani A, Furukawa TA, Salanti G, Chaimani A, Atkinson LZ, Ogawa Y, et al. Comparative efficacy and acceptability of 21 antidepressant drugs for the acute treatment of adults with major depressive disorder: a systematic review and network meta-analysis. The Lancet. 2018 Apr 7;391(10128):1357–66. doi:10.1016/S0140-6736(17)32802-7 PubMed PMID: 29477251.

6. Jakubovski E, Varigonda AL, Freemantle N, Taylor MJ, Bloch MH. Systematic Review and Meta-Analysis: Dose-Response Relationship of Selective-Serotonin Reuptake Inhibitors in Major Depressive Disorder. Am J Psychiatry. 2016 Feb 1;173(2):174–83. doi:10.1176/appi.ajp.2015.15030331 PubMed PMID: 26552940; PubMed Central PMCID: PMC4975858.

7. Moncrieff J, Cooper RE, Stockmann T, Amendola S, Hengartner MP, Horowitz MA. The serotonin theory of depression: a systematic umbrella review of the evidence. Mol Psychiatry. 2022 Jul 20;1–14. doi:10.1038/s41380-022-01661-0

8. Malhi GS, Mann JJ. Depression. Lancet. 2018/11/07 edn. 2018 Nov 24;392(10161):2299–312. Located at: 30396512. doi:10.1016/s0140-6736(18)31948-2

9. Wong DT, Horng JS, Bymaster FP. A selective inhibitor of serotonin uptake: lilly 110140, 3-(p-trifluoromethylphenoxy)-N-methyl-3-phenylpropylamine. Life Sci. 1974;15(3):471–9.

10. Mosienko V, Bert B, Beis D, Matthes S, Fink H, Bader M, et al. Exaggerated aggression and decreased anxiety in mice deficient in brain serotonin. Transl Psychiatry. 2012 May;2(5):e122–e122. doi:10.1038/tp.2012.44

11. Angoa-Pérez M, Kane MJ, Briggs DI, Herrera-Mundo N, Sykes CE, Francescutti DM, et al. Mice genetically depleted of brain serotonin do not display a depression-like behavioral phenotype. ACS Chem Neurosci. 2014 Oct 15;5(10):908–19. doi:10.1021/cn500096g PubMed PMID: 25089765; PubMed Central PMCID: PMC4777283.

12. Mosienko V, Beis D, Pasqualetti M, Waider J, Matthes S, Qadri F, et al. Life without brain serotonin: reevaluation of serotonin function with mice deficient in brain serotonin

bioRxiv preprint doi: https://doi.org/10.64898/2026.06.04.730071; this version posted June 8, 2026. The copyright holder for this preprint (which was not certified by peer review) is the author/funder, who has granted bioRxiv a license to display the preprint in perpetuity. It is made available under a CC-BY 4.0 International license.

synthesis. Behav Brain Res. 2015 Jan 15;277:78–88. doi:10.1016/j.bbr.2014.06.005 PubMed PMID: 24928769.

13. Diaz SL, Doly S, Narboux-Nême N, Fernández S, Mazot P, Banas SM, et al. 5-HT(2B) receptors are required for serotonin-selective antidepressant actions. Mol Psychiatry. 2012 Feb;17(2):154–63. doi:10.1038/mp.2011.159 PubMed PMID: 22158014; PubMed Central PMCID: PMC3381222.

14. Diaz SL, Narboux-Nême N, Boutourlinsky K, Doly S, Maroteaux L. Mice lacking the serotonin 5-HT2B receptor as an animal model of resistance to selective serotonin reuptake inhibitors antidepressants. Eur Neuropsychopharmacol. 2016 Feb;26(2):265–79. doi:10.1016/j.euroneuro.2015.12.012 PubMed PMID: 26727039.

15. Czéh B, Simon M, Schmelting B, Hiemke C, Fuchs E. Astroglial Plasticity in the Hippocampus is Affected by Chronic Psychosocial Stress and Concomitant Fluoxetine Treatment. Neuropsychopharmacol. 2006 Aug;31(8):1616–26. doi:10.1038/sj.npp.1300982

16. Shu X, Sun Y, Sun X, Zhou Y, Bian Y, Shu Z, et al. The effect of fluoxetine on astrocyte autophagy flux and injured mitochondria clearance in a mouse model of depression. Cell Death Dis. 2019 Aug 2;10(8):577. Located at: 31371719. doi:10.1038/s41419-019-1813-9

17. Chen B, Zhang M, Ji M, Gong W, Chen B, Zorec R, et al. The Association Between Antidepressant Effect of SSRIs and Astrocytes: Conceptual Overview and Meta-analysis of the Literature. Neurochem Res. 2021 Oct 1;46(10):2731–45. doi:10.1007/s11064-020-03225-6

18. Cobb JA, O'Neill K, Milner J, Mahajan GJ, Lawrence TJ, May WL, et al. Density of GFAP-immunoreactive astrocytes is decreased in left hippocampi in major depressive disorder. Neuroscience. 2016 Mar 1;316:209–20. Located at: 26742791. doi:10.1016/j.neuroscience.2015.12.044

19. Rajkowska G, Legutko B, Moulana M, Syed M, Romero DG, Stockmeier CA, et al. Astrocyte pathology in the ventral prefrontal white matter in depression. Journal of Psychiatric Research. 2018 Jul 1;102:150–8. doi:10.1016/j.jpsychires.2018.04.005

20. Nibuya M, Nestler EJ, Duman RS. Chronic antidepressant administration increases the expression of cAMP response element binding protein (CREB) in rat hippocampus. The Journal of neuroscience : the official journal of the Society for Neuroscience. 1996/04/01 edn. 1996 Apr 1;16(7):2365–72. Located at: 8601816. doi:10.1523/jneurosci.16-07-02365.1996

21. Donati RJ, Rasenick MM. G protein signaling and the molecular basis of antidepressant action. Life Sciences. 2003 May 23;73(1):1–17. doi:10.1016/S0024-3205(03)00249-2

22. Virok DP, Kis Z, Szegedi V, Juhász G, Zvara A, Müller G, et al. Functional changes in transcriptomes of the prefrontal cortex and hippocampus in a mouse model of anxiety. Pharmacol Rep. 2011;63(2):348–61. doi:10.1016/s1734-1140(11)70501-1 PubMed PMID: 21602590.

23. Verma P, Shakya M. Transcriptomics and sequencing analysis of gene expression profiling for major depressive disorder. Indian J Psychiatry. 2021;63(6):549–53. doi:10.4103/psychiatry.IndianJPsychiatry_858_20 PubMed PMID: 35136251; PubMed Central PMCID: PMC8793711.

bioRxiv preprint doi: https://doi.org/10.64898/2026.06.04.730071; this version posted June 8, 2026. The copyright holder for this preprint (which was not certified by peer review) is the author/funder, who has granted bioRxiv a license to display the preprint in perpetuity. It is made available under a CC-BY 4.0 International license.

24. Donati RJ, Schappi J, Czysz AH, Jackson A, Rasenick MM. Differential effects of antidepressants escitalopram versus lithium on Gs alpha membrane relocalization. BMC Neurosci. 2015 Jul 11;16:40. doi:10.1186/s12868-015-0178-y PubMed PMID: 26162823; PubMed Central PMCID: PMC4499192.

25. Thome J, Sakai N, Shin K, Steffen C, Zhang YJ, Impey S, et al. cAMP response element-mediated gene transcription is upregulated by chronic antidepressant treatment. The Journal of neuroscience : the official journal of the Society for Neuroscience. 2000/05/20 edn. 2000 Jun 1;20(11):4030–6. Located at: 10818138. doi:10.1523/jneurosci.20-11-04030.2000

26. Takano K, Yamasaki H, Kawabe K, Moriyama M, Nakamura Y. Imipramine induces brain-derived neurotrophic factor mRNA expression in cultured astrocytes. J Pharmacol Sci. 2012;120(3):176–86. doi:10.1254/jphs.12039fp PubMed PMID: 23076128.

27. Wray NH, Schappi JM, Singh H, Senese NB, Rasenick MM. NMDAR-independent, cAMP-dependent antidepressant actions of ketamine. Mol Psychiatry. 2018/06/14 edn. 2019 Dec;24(12):1833–43. Located at: 29895894. doi:10.1038/s41380-018-0083-8

28. Erb SJ, Schappi JM, Rasenick MM. Antidepressants Accumulate in Lipid Rafts Independent of Monoamine Transporters to Modulate Redistribution of the G Protein, Gαs. J Biol Chem. 2016 Sep 16;291(38):19725–33. doi:10.1074/jbc.M116.727263 PubMed PMID: 27432886; PubMed Central PMCID: PMC5025664.

29. Donati RJ, Thukral C, Rasenick MM. Chronic treatment of C6 glioma cells with antidepressant drugs results in a redistribution of Gsalpha. Mol Pharmacol. 2001 Jun;59(6):1426–32. doi:10.1124/mol.59.6.1426 PubMed PMID: 11353802.

30. Kinoshita M, Hirayama Y, Fujishita K, Shibata K, Shinozaki Y, Shigetomi E, et al. Anti-Depressant Fluoxetine Reveals its Therapeutic Effect Via Astrocytes. EBioMedicine. 2018 Jun;32:72–83. doi:10.1016/j.ebiom.2018.05.036 PubMed PMID: 29887330; PubMed Central PMCID: PMC6020856.

31. Vaccari Cardoso B, Shevelkin AV, Terrillion C, Mychko O, Mosienko V, Kasparov S, et al. Reducing l-lactate release from hippocampal astrocytes by intracellular oxidation increases novelty induced activity in mice. Glia. 2021/01/06 edn. 2021 Jan 5. Located at: 33400321. doi:10.1002/glia.23960

32. Henry ME, Schmidt ME, Hennen J, Villafuerte RA, Butman ML, Tran P, et al. A Comparison of Brain and Serum Pharmacokinetics of R-Fluoxetine and Racemic Fluoxetine: A 19-F MRS Study. Neuropsychopharmacol. 2005 Aug;30(8):1576–83. doi:10.1038/sj.npp.1300749

33. Karson CN, Newton JE, Livingston R, Jolly JB, Cooper TB, Sprigg J, et al. Human brain fluoxetine concentrations. J Neuropsychiatry Clin Neurosci. 1993;5(3):322–9. doi:10.1176/jnp.5.3.322 PubMed PMID: 8369643.

34. Johnson RD, Lewis RJ, Angier MK. The distribution of fluoxetine in human fluids and tissues. J Anal Toxicol. 2007 Sep;31(7):409–14. doi:10.1093/jat/31.7.409 PubMed PMID: 17725889.

35. Allaman I, Fiumelli H, Magistretti PJ, Martin JL. Fluoxetine regulates the expression of neurotrophic/growth factors and glucose metabolism in astrocytes. Psychopharmacology. 2011/02/09 edn. 2011 Jul;216(1):75–84. Located at: 21301813. doi:10.1007/s00213-011-2190-y

bioRxiv preprint doi: https://doi.org/10.64898/2026.06.04.730071; this version posted June 8, 2026. The copyright holder for this preprint (which was not certified by peer review) is the author/funder, who has granted bioRxiv a license to display the preprint in perpetuity. It is made available under a CC-BY 4.0 International license.

36. Shu X, Sun Y, Sun X, Zhou Y, Bian Y, Shu Z, et al. The effect of fluoxetine on astrocyte autophagy flux and injured mitochondria clearance in a mouse model of depression. Cell Death Dis. 2019 Aug 2;10(8):577. doi:10.1038/s41419-019-1813-9 PubMed PMID: 31371719; PubMed Central PMCID: PMC6675792.

37. Klarenbeek J, Goedhart J, van Batenburg A, Groenewald D, Jalink K. Fourth-generation epac-based FRET sensors for cAMP feature exceptional brightness, photostability and dynamic range: characterization of dedicated sensors for FLIM, for ratiometry and with high affinity. PloS one. 2015/04/16 edn. 2015;10(4):e0122513. Located at: 25875503. doi:10.1371/journal.pone.0122513

38. Thestrup T, Litzlbauer J, Bartholomäus I, Mues M, Russo L, Dana H, et al. Optimized ratiometric calcium sensors for functional in vivo imaging of neurons and T lymphocytes. Nat Methods. 20140105th edn. 2014 Feb;11(2):175–82. Located at: 24390440. doi:10.1038/nmeth.2773

39. Wu Z, He K, Chen Y, Li H, Pan S, Li B, et al. A sensitive GRAB sensor for detecting extracellular ATP in vitro and in vivo. Neuron. 2022 Mar 2;110(5):770-782.e5. doi:10.1016/j.neuron.2021.11.027 PubMed PMID: 34942116.

40. Endo F, Kasai A, Soto JS, Yu X, Qu Z, Hashimoto H, et al. Molecular basis of astrocyte diversity and morphology across the CNS in health and disease. Science. 2022 Nov 4;378(6619):eadc9020. doi:10.1126/science.adc9020 PubMed PMID: 36378959; PubMed Central PMCID: PMC9873482.

41. Theparambil SM, Kopach O, Braga A, Nizari S, Hosford PS, Sagi-Kiss V, et al. Adenosine signalling to astrocytes coordinates brain metabolism and function. Nature. 2024 Jul 3;1–8. doi:10.1038/s41586-024-07611-w

42. Zhang S, Li B, Lovatt D, Xu J, Song D, Goldman SA, et al. 5-HT2B receptors are expressed on astrocytes from brain and in culture and are a chronic target for all five conventional 'serotonin-specific reuptake inhibitors'. Neuron Glia Biology. 2010 May;6(2):113–25. doi:10.1017/S1740925X10000141

43. Zhang Y, Sloan SA, Clarke LE, Caneda C, Plaza CA, Blumenthal PD, et al. Purification and Characterization of Progenitor and Mature Human Astrocytes Reveals Transcriptional and Functional Differences with Mouse. Neuron. 2016 Jan 6;89(1):37–53. doi:10.1016/j.neuron.2015.11.013 PubMed PMID: 26687838.

44. Allard B, Longhi MS, Robson SC, Stagg J. The ectonucleotidases CD39 and CD73: novel checkpoint inhibitor targets. Immunol Rev. 2017 Mar;276(1):121–44. doi:10.1111/imr.12528 PubMed PMID: 28258700; PubMed Central PMCID: PMC5338647.

45. Badimon A, Strasburger HJ, Ayata P, Chen X, Nair A, Ikegami A, et al. Negative feedback control of neuronal activity by microglia. Nature. 2020 Oct;586(7829):417–23. doi:10.1038/s41586-020-2777-8

46. Schmuck K, Ullmer C, Engels P, Lübbert H. Cloning and functional characterization of the human 5-HT2B serotonin receptor. FEBS Lett. 1994 Mar 28;342(1):85–90. doi:10.1016/0014-5793(94)80590-3 PubMed PMID: 8143856.

bioRxiv preprint doi: https://doi.org/10.64898/2026.06.04.730071; this version posted June 8, 2026. The copyright holder for this preprint (which was not certified by peer review) is the author/funder, who has granted bioRxiv a license to display the preprint in perpetuity. It is made available under a CC-BY 4.0 International license.

47. Li B, Zhang S, Zhang H, Nu W, Cai L, Hertz L, et al. Fluoxetine-mediated 5-HT2B receptor stimulation in astrocytes causes EGF receptor transactivation and ERK phosphorylation. Psychopharmacology. 2008 Dec;201(3):443–58. doi:10.1007/s00213-008-1306-5

48. Li B, Zhang S, Li M, Hertz L, Peng L. Chronic treatment of astrocytes with therapeutically relevant fluoxetine concentrations enhances cPLA2 expression secondary to 5-HT2B-induced, transactivation-mediated ERK1/2 phosphorylation. Psychopharmacology (Berl). 2009 Nov;207(1):1–12. doi:10.1007/s00213-009-1631-3 PubMed PMID: 19662385.

49. Liu Y, Wang Z, Li J, Ban Y, Mao G, Zhang M, et al. Inhibition of 5-Hydroxytryptamine Receptor 2B Reduced Vascular Restenosis and Mitigated the β-Arrestin2-Mammalian Target of Rapamycin/p70S6K Pathway. J Am Heart Assoc. 2018 Jan 30;7(3):e006810. doi:10.1161/JAHA.117.006810 PubMed PMID: 29382665; PubMed Central PMCID: PMC5850233.

50. Nebigil CG, Etienne N, Messaddeq N, Maroteaux L. Serotonin is a novel survival factor of cardiomyocytes: mitochondria as a target of 5-HT2B receptor signaling. FASEB J. 2003 Jul;17(10):1373–5. doi:10.1096/fj.02-1122fje PubMed PMID: 12738797.

51. Mastitskaya S, Turovsky E, Marina N, Theparambil SM, Hadjihambi A, Kasparov S, et al. Astrocytes Modulate Baroreflex Sensitivity at the Level of the Nucleus of the Solitary Tract. J Neurosci. 2020 Apr 8;40(15):3052–62. doi:10.1523/JNEUROSCI.1438-19.2020 PubMed PMID: 32132265.

52. Sjöstedt E, Zhong W, Fagerberg L, Karlsson M, Mitsios N, Adori C, et al. An atlas of the protein-coding genes in the human, pig, and mouse brain. Science. 2020 Mar 6;367(6482):eaay5947. doi:10.1126/science.aay5947

53. The Human Protein Atlas [Internet]. 2026 [cited 2026 Jan 31]. Available from: https://www.proteinatlas.org/

54. Fang Y, Ding X, Zhang Y, Cai L, Ge Y, Ma K, et al. Fluoxetine inhibited the activation of A1 reactive astrocyte in a mouse model of major depressive disorder through astrocytic 5-HT2BR/β-arrestin2 pathway. J Neuroinflammation. 2022 Jan 29;19(1):23. doi:10.1186/s12974-022-02389-y PubMed PMID: 35093099; PubMed Central PMCID: PMC8800238.

55. Li H, Zhao Y, Dai R, Geng P, Weng D, Wu W, et al. Astrocytes release ATP/ADP and glutamate in flashes via vesicular exocytosis. Mol Psychiatry. 2025 Jun;30(6):2475–89. doi:10.1038/s41380-024-02851-8

56. Wang ML, Song YL, Wu DY, Li H, Li ZM, Xiong XX, et al. Astrocytic connexin43 in the medial prefrontal cortex regulates depressive- and anxiety-like behaviors via ATP release. Pharmacological Research. 2025 Jul 1;217:107798. doi:10.1016/j.phrs.2025.107798

57. Lin S, Huang L, Luo Z cai, Li X, Jin S yang, Du Z jun, et al. The ATP Level in the Medial Prefrontal Cortex Regulates Depressive-like Behavior via the Medial Prefrontal Cortex-Lateral Habenula Pathway. Biological Psychiatry. 2022 Aug 1;From Molecules to Circuits in Depression92(3):179–92. doi:10.1016/j.biopsych.2022.02.014

58. Cao X, Li LP, Wang Q, Wu Q, Hu HH, Zhang M, et al. Astrocyte-derived ATP modulates depressive-like behaviors. Nat Med. 2013 Jun;19(6):773–7. Located at: 23644515. doi:10.1038/nm.3162

bioRxiv preprint doi: https://doi.org/10.64898/2026.06.04.730071; this version posted June 8, 2026. The copyright holder for this preprint (which was not certified by peer review) is the author/funder, who has granted bioRxiv a license to display the preprint in perpetuity. It is made available under a CC-BY 4.0 International license.

59. Hertz L, Rothman DL, Li B, Peng L. Chronic SSRI stimulation of astrocytic 5-HT2B receptors change multiple gene expressions/editings and metabolism of glutamate, glucose and glycogen: a potential paradigm shift. Front Behav Neurosci. 2015;9:25. doi:10.3389/fnbeh.2015.00025 PubMed PMID: 25750618; PubMed Central PMCID: PMC4335176.

60. Schneider E, Rissiek A, Winzer R, Puig B, Rissiek B, Haag F, et al. Generation and Function of Non-cell-bound CD73 in Inflammation. Front Immunol. 2019 Jul 26;10. doi:10.3389/fimmu.2019.01729

61. Dragić M, Mitrović N, Adžić M, Nedeljković N, Grković I. Microglial- and Astrocyte-Specific Expression of Purinergic Signaling Components and Inflammatory Mediators in the Rat Hippocampus During Trimethyltin-Induced Neurodegeneration. ASN Neuro. 2021 Jan 1;13:17590914211044882. doi:10.1177/17590914211044882

62. Yue C, Wang N, Zhai H, Yuan Z, Cui Y, Quan J, et al. Adenosine signalling drives antidepressant actions of ketamine and ECT. Nature. 2026 Jan;649(8096):423–31. doi:10.1038/s41586-025-09755-9

63. Karson CN, Newton JE, Livingston R, Jolly JB, Cooper TB, Sprigg J, et al. Human brain fluoxetine concentrations. The Journal of neuropsychiatry and clinical neurosciences. 1993/01/01 edn. 1993 Summer;5(3):322–9. Located at: 8369643. doi:10.1176/jnp.5.3.322

64. Amsterdam JD. Fluoxetine and norfluoxetine plasma concentrations in major depression: a multicenter study. AJP. 1997 Jul;154(7):963–9. doi:10.1176/ajp.154.7.963

65. Bonhaus DW, Bach C, DeSouza A, Salazar FHR, Matsuoka BD, Zuppan P, et al. The pharmacology and distribution of human 5-hydroxytryptamine2B (5-HT2b) receptor gene products: comparison with 5-HT2a and 5-HT2c receptors. British Journal of Pharmacology. 1995;115(4):622–8. doi:10.1111/j.1476-5381.1995.tb14977.x

66. Knight AR, Misra A, Quirk K, Benwell K, Revell D, Kennett G, et al. Pharmacological characterisation of the agonist radioligand binding site of 5-HT2A, 5-HT2B and 5-HT2C receptors. Naunyn-Schmiedeberg's Arch Pharmacol. 2004 Aug 1;370(2):114–23. doi:10.1007/s00210-004-0951-4

67. Kreisel T, Frank MG, Licht T, Reshef R, Ben-Menachem-Zidon O, Baratta MV, et al. Dynamic microglial alterations underlie stress-induced depressive-like behavior and suppressed neurogenesis. Mol Psychiatry. 2014 Jun;19(6):699–709. doi:10.1038/mp.2013.155 PubMed PMID: 24342992.

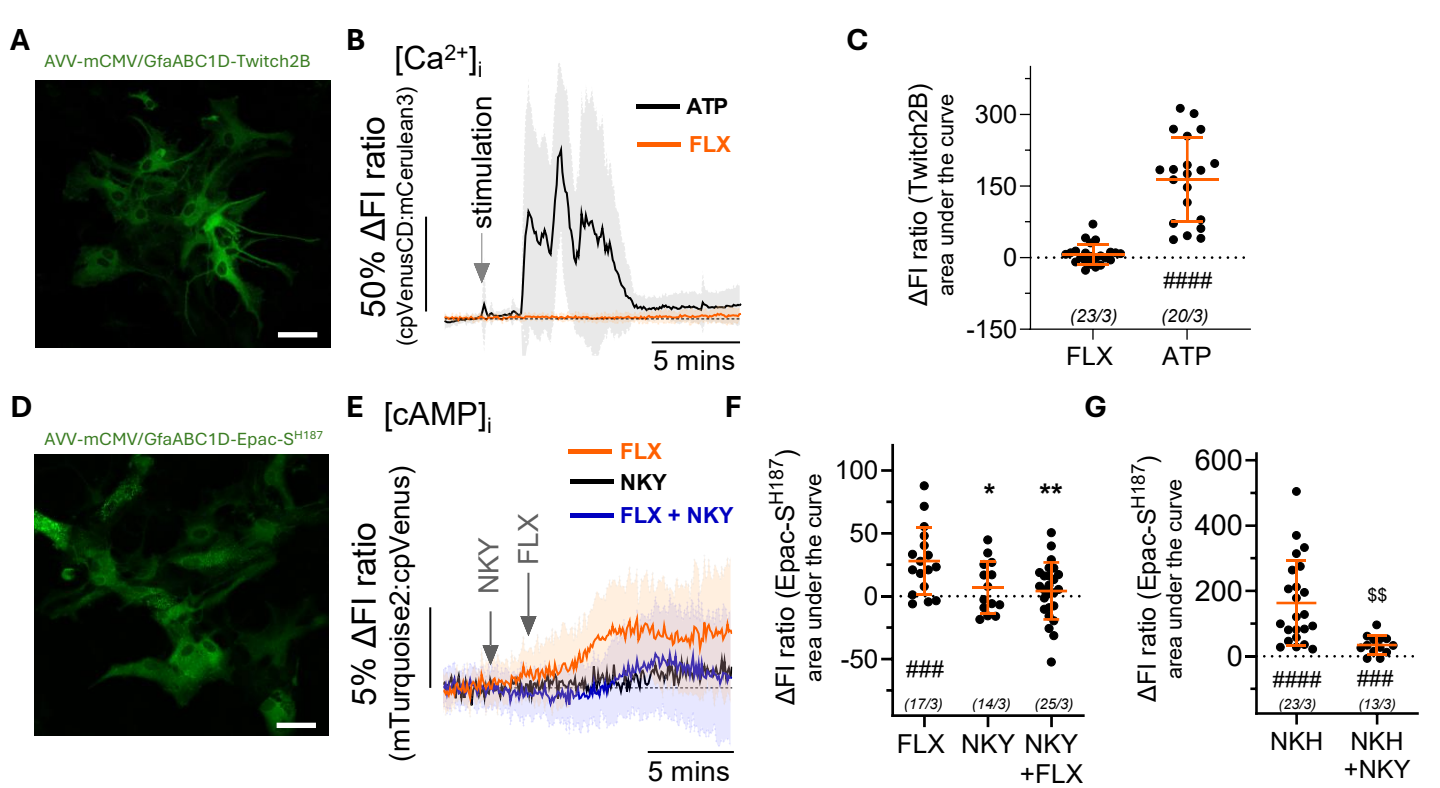
68. Stein DJ, Vasconcelos MF, Albrechet-Souza L, Ceresér KMM, de Almeida RMM. Microglial Over-Activation by Social Defeat Stress Contributes to Anxiety- and Depressive-Like Behaviors. Front Behav Neurosci. 2017 Oct 24;11. doi:10.3389/fnbeh.2017.00207

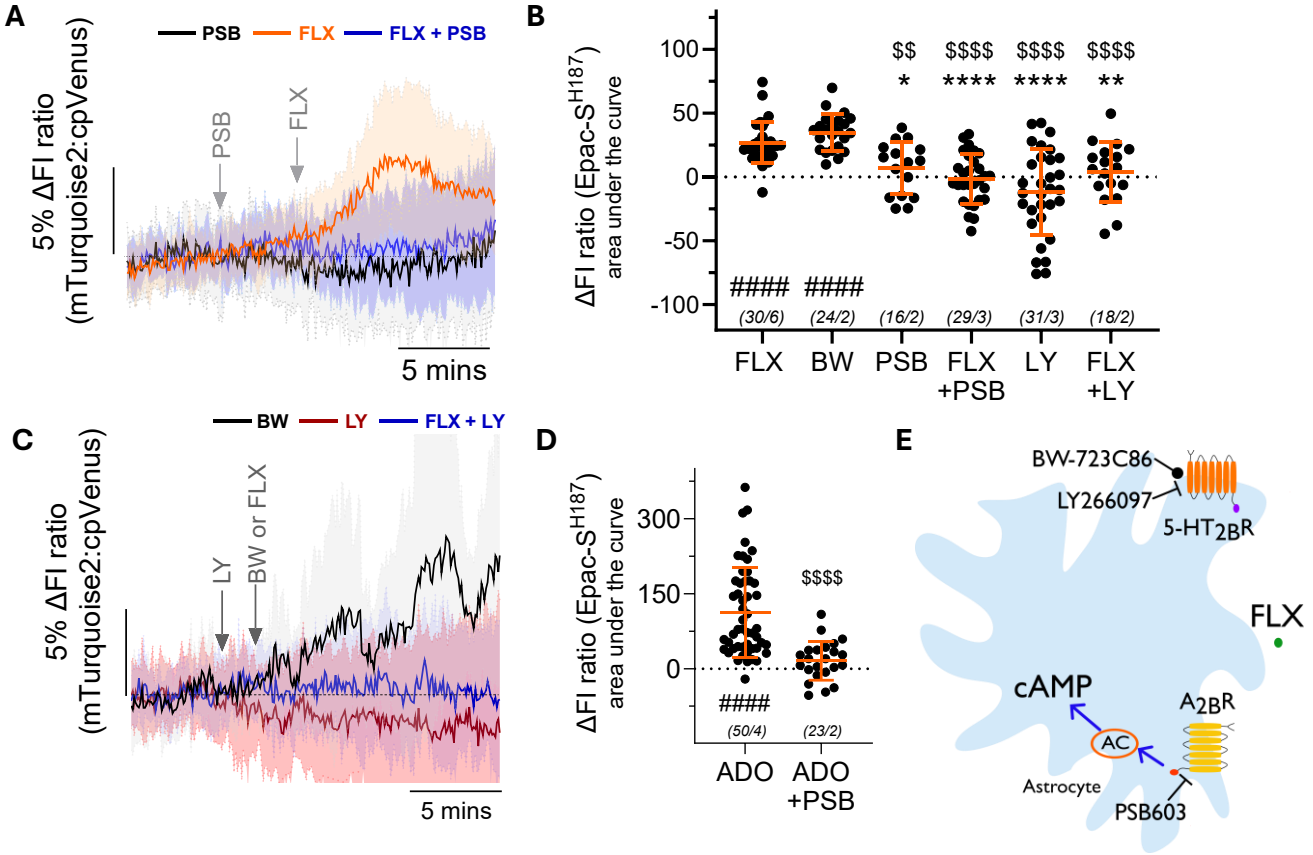
69. Setiawan E, Attwells S, Wilson AA, Mizrahi R, Rusjan PM, Miler L, et al. Association of translocator protein total distribution volume with duration of untreated major depressive disorder: a cross-sectional study. Lancet Psychiatry. 2018 Apr;5(4):339–47. doi:10.1016/S2215-0366(18)30048-8 PubMed PMID: 29496589.

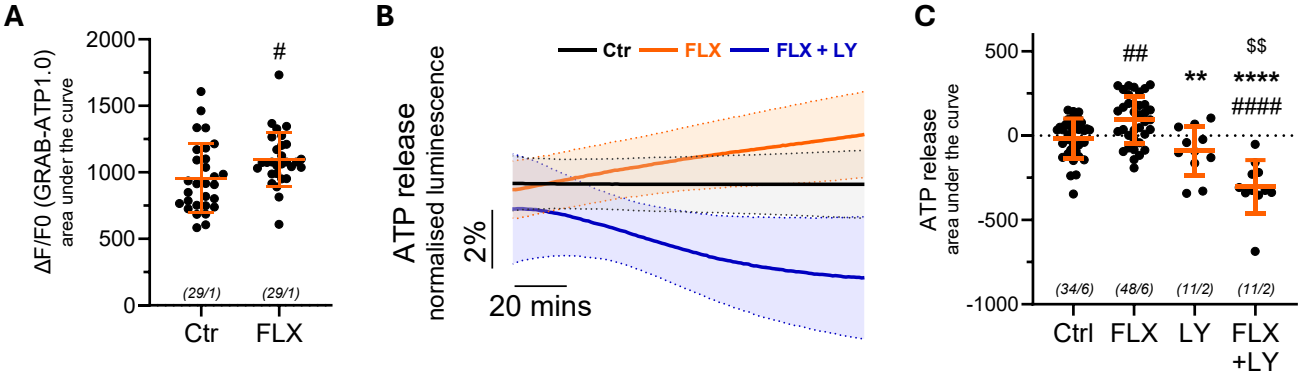
70. Setiawan E, Wilson AA, Mizrahi R, Rusjan PM, Miler L, Rajkowska G, et al. Role of translocator protein density, a marker of neuroinflammation, in the brain during major depressive episodes. JAMA Psychiatry. 2015 Mar;72(3):268–75.

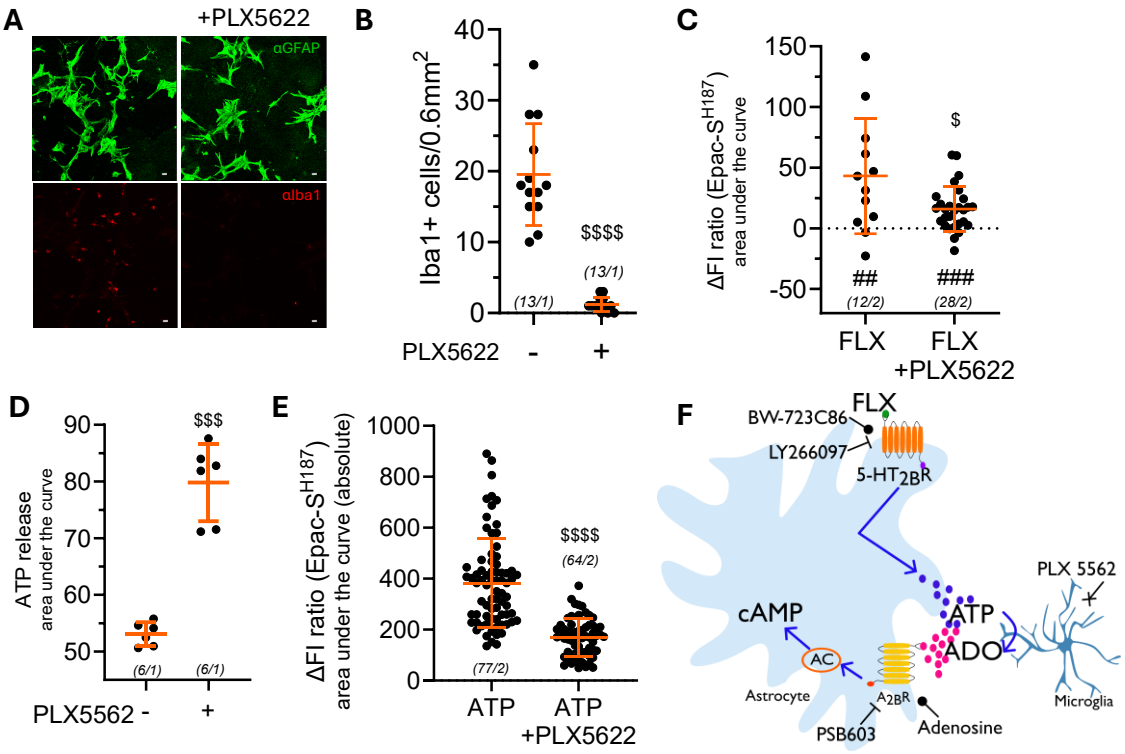
bioRxiv preprint doi: https://doi.org/10.64898/2026.06.04.730071; this version posted June 8, 2026. The copyright holder for this preprint (which was not certified by peer review) is the author/funder, who has granted bioRxiv a license to display the preprint in perpetuity. It is made available under a CC-BY 4.0 International license.

doi:10.1001/jamapsychiatry.2014.2427 PubMed PMID: 25629589; PubMed Central PMCID: PMC4836849.


A
AVV-mCMV/GfaABC1D-Twitch2B
B
[Ca2+]i
50% ΔFI ratio
(cpVenusCD:mCerulean3)
stimulation
ATP
FLX
5 mins
C
ΔFI ratio (Twitch2B)
area under the curve
300
150
0
-150
####
(23/3)
(20/3)
FLX
ATP
D
AVV-mCMV/GfaABC1D-Epac-SH187
E
[cAMP]i
5% ΔFI ratio
(mTurquoise2:cpVenus)
FLX
NKY
FLX + NKY
NKY
FLX
5 mins
F
ΔFI ratio (Epac-SH187)
area under the curve
100
50
0
-50
*
**
###
(17/3)
(14/3)
(25/3)
FLX
NKY
NKY +FLX
G
ΔFI ratio (Epac-SH187)
area under the curve
600
400
200
0
$$
####
###
(23/3)
(13/3)
NKH
NKH +NKY


A
PSB
FLX
FLX + PSB
5% ΔFI ratio (mTurquoise2:cpVenus)
PSB
FLX
5 mins
B
ΔFI ratio (Epac-S^H187) area under the curve
100
50
0
-50
-100
$$
$$$$
$$$$
$$$$
*
****
****
**
####
####
(30/6)
(24/2)
(16/2)
(29/3)
(31/3)
(18/2)
FLX
BW
PSB
FLX +PSB
LY
FLX +LY
C
BW
LY
FLX + LY
5% ΔFI ratio (mTurquoise2:cpVenus)
LY
BW or FLX
5 mins
D
ΔFI ratio (Epac-S^H187) area under the curve
300
150
0
$$$$
####
(50/4)
(23/2)
ADO
ADO +PSB
E
BW-723C86
LY266097
5-HT2BR
FLX
cAMP
AC
A2BR
Astrocyte
PSB603


A
ΔF/F0 (GRAB-ATP1.0)
area under the curve
2000
1500
1000
500
0
#
(29/1)
(29/1)
Ctr
FLX
B
Ctr
FLX
FLX + LY
ATP release
normalised luminescence
2%
20 mins
C
ATP release
area under the curve
500
0
-500
-1000
##
**
$$
****
####
(34/6)
(48/6)
(11/2)
(11/2)
Ctrl
FLX
LY
FLX
+LY


A
+PLX5622
αGFAP
αIba1
B
Iba1+ cells/0.6mm2
40
30
20
10
0
$$$$
(13/1)
(13/1)
PLX5622 - +
C
ΔFI ratio (Epac-SH187)
area under the curve
150
100
50
0
-50
$
##
###
(12/2)
(28/2)
FLX
FLX
+PLX5622
D
ATP release
area under the curve
90
80
70
60
50
$$$
(6/1)
(6/1)
PLX5562 - +
E
ΔFI ratio (Epac-SH187)
area under the curve (absolute)
1000
800
600
400
200
0
$$$$
(64/2)
(77/2)
ATP
ATP
+PLX5622
F
FLX
BW-723C86
LY266097
5-HT2BR
PLX 5562
cAMP
ATP
ADO
AC
Astrocyte
A2BR
PSB603
Adenosine
Microglia